Robust Iterative Learning for High Precision Motion Control through $\mathcal{L}_1$ Adaptive Feedback

Berk Altın[a,*], Kira Barton[b]

[a]*Department of Electrical Engineering and Computer Science, University of Michigan, Ann Arbor, MI 48109, USA*
[b]*Department of Mechanical Engineering, University of Michigan, Ann Arbor, MI 48109, USA*

Abstract

The diversity of precision motion control applications and their demanding design specifications pose a large array of control challenges. Hence, precision motion control design relies on a variety of advanced control strategies developed to cope with specific problems present in control theory. A popular feedforward control technique for repetitive systems is iterative learning control (ILC). While ILC can decrease tracking errors up to several orders of magnitude, the achievable performance is limited by dynamic uncertainty. We propose the combination of $\mathcal{L}_1$ adaptive control ($\mathcal{L}_1$ AC) and linear ILC for precision motion control under parametric uncertainties. We rely on the adaptive loop to compensate for parametric uncertainties, and ensure that the plant uncertainty is sufficiently small so that an aggressive learning controller can be designed on the nominal system. We exploit the closed loop stability condition of $\mathcal{L}_1$ AC to design simple, robust ILC update laws that reduce tracking errors to measurement noise for time varying references and uncertainties. We demonstrate in simulation that the combined control scheme maintains a highly predictable, monotonic system behavior; and achieves near perfect tracking within a few trials regardless of the uncertainty present.

Keywords: adaptive control, iterative learning control, robust control, parametric uncertainty, monotonic convergence

1. Introduction

Iterative learning control (ILC) is a feedforward control strategy for systems that execute the same task repeatedly over a finite time horizon [1]. ILC is based on the idea that the tracking performance of such systems can be improved by using information from previous trials. Contrary to other learning type control strategies (e.g. adaptive control, neural networks, repetitive control), ILC modifies the input signal rather than the controller [2]. In a way, ILC is a form of feedback control over the iteration domain. Consistent with this property, iterative learning controllers offer simplicity, robustness and fast convergence to iteration domain equilibria with performance improvements up to several orders of magnitude over conventional control strategies.

One of the essential challenges that motivates the field of ILC is dynamic uncertainty. Much as in feedback control, the main approaches for mitigating uncertainy can be roughly classified as robust or adaptive methods. Considerable research has been done on the synthesis of ILC algorithms that are robust to exogenous disturbances, stochastic effects, interval uncertainties, and high frequency modeling uncertainties (see [1, 3] and references therein). References [4–6] provide good examples of $\mathcal{H}_\infty$ methods for finite and infinite horizon cases; an area in which much work has been done. In [7], the combination of $\mathcal{H}_\infty$ feedback control with ILC was analyzed, with the premise of bandwidth separated repetitive and nonrepetitive exogenous signals. One particular example that underlines parametric uncertainties from a robustness perspective is [8], in which stability of ILC to interval uncertainties in the impulse response is evaluated. The drawback to these methods is that while ILC convergence is guaranteed within the prescribed set of uncertainties, performance is often limited due to conservative designs. Additionally, the sensitivity of robust learning controllers to variations in the uncertainties is still an open question.

Parametric uncertainties have similarly been studied

*Corresponding author.
Email addresses: altin@umich.edu (Berk Altın), bartonkl@umich.edu (Kira Barton)

extensively in the adaptive ILC setting with special attention to the application area of robotics, wherein iterative estimation schemes were used to augment the feedback controllers using Lyapunov like methods [9, 10]. Iterative estimation was also used to reduce the model tracking error and improve transient response in model reference adaptive control (MRAC) [11–13]. Other works showed how adaptive feedback control methods can be extended to ILC in a straightforward way[14], and proved universal adaptive ILC laws for single-input single-output (SISO) linear time invariant (LTI) systems with nonzero first Markov parameters [15]. While the adaptive nature of these systems signify high performance and reduced sensitivity to parametric variations, the robustness of adaptive ILC to unmodeled dynamics may be questionable, analogous to adaptive feedback control [16, 17].

Most of the fundamental limitations and trade-offs of control theory can be observed to a greater extent in precision motion control due to complex, demanding design specifications. Key issues in the control of precision positioning systems include robustness to parameter variations, unmodeled high frequency dynamics, and the bandwidth-precision trade-off [18]. More complex process modeling can mitigate uncertainty issues to an extent, but this becomes unfeasible as complexity increases, specifically due to the fact that certain information about the process, such as external loads and/or parameters that are sensitive to exogenous effects, cannot be known a priori. Although adaptive feedback methods provide a good solution to the problem of *robustness to parametric variation* and increase precision, this often comes at the expense of *reduced robustness to unmodeled dynamics* [17] as fast estimation, which is desired from a performance standpoint, leads to high gain feedback. This problem essentially boils down to the fact that conventional adaptive control ignores Bode's sensitivity integral [19, 20], also known as the *waterbed effect*, by compensating for uncertainties throughout the whole frequency spectrum. Similarly, while ILC extends the *available bandwidth* [20] of the control channel for repetitive systems, thereby alleviating the bandwidth-precision trade-off, the achievable reduction in errors and monotonicity on the iteration axis depends largely on the level of uncertainty in the feedback stabilized plant.

To address these issues, this work combines conventional ILC with $\mathcal{L}_1$ adaptive feedback control, and is an extension of our previous work in [21–23]. $\mathcal{L}_1$ adaptive control ($\mathcal{L}_1$ AC) is a recent MRAC paradigm that bridges the gap between adaptive and robust control with a priori known, quantifiable transient response *and* robustness bounds [17]. The idea of combining ILC with $\mathcal{L}_1$ AC was first introduced in [21], wherein the adaptive loop was utilized to keep the plant sensitivity close to its nominal value for performance improvement through learning. Despite the displayed advantages of $\mathcal{L}_1$ AC over linear feedback, a trade-off was observed between the closed loop bandwidth and learning performance. More precisely, it was seen that higher closed loop bandwidths resulted in slower convergence and larger converged errors in the iteration domain. To resolve this problem, we proposed the augmentation of the $\mathcal{L}_1$ AC architecture with an arbitrary feedforward signal to accommodate learning, leading to an adaptation that considers changes in the nominal system behavior due to learning [22]. The resulting $\mathcal{L}_1$ AC-ILC ($\mathcal{L}_1$-ILC) scheme had predictable performance in both the time and iteration domains: The feedforward augmented closed loop preserved the a priori known quantifiable transients from $\mathcal{L}_1$ AC theory, and the learning controller displayed similar convergence behavior regardless of the uncertainty present in the system. It was also seen that increasing feedback bandwidths resulted in decreasing effects of uncertainty in the iteration domain, with faster convergence and lower converged errors. In [23], we presented design guidelines and showed the performance gains of the modified scheme over linear output feedback on a large range nanopositioner via simulation. The main differences between this work and our previous work include:

1. A generalized approach to $\mathcal{L}_1$-ILC for different classes of linear systems through vector space methods
2. Extension of the robust monotonic learning convergence results to time varying parametric uncertainties
3. Design guidelines for the $\mathcal{L}_1$-ILC scheme that link feedback-learning filter designs to classical control ideas, and show how the $\mathcal{L}_1$ AC stability condition can be satisfied for a given system
4. Validation of the performance improvements of the proposed scheme in comparison with an LTI feedback based ILC, through extensive simulations on a precision positioning system subject to time varying parametric uncertainties

Our work differs from the existing literature in several ways: First, as we have mentioned, previous work on adaptive methods in learning have focused on *adaptive ILC*, wherein adaptive learning laws are considered with or without adaptive feedback. Second, adaptive feedback has not been used in a robust ILC setting before.

Third, although the idea of combining ILC with advanced feedback methods to achieve better performance is not new, to the best of our knowledge, the combination of conventional ILC with adaptive feedback has not been employed before.

In this paper, we demonstrate how ILC algorithms can be combined with $\mathcal{L}_1$ AC schemes to achieve robust, high precision motion control. We present feedforward augmented $\mathcal{L}_1$ AC architectures for state and output feedback cases (see figures 2 and 5) to accommodate parallel ILC signals and show how this preserves the a priori known $\mathcal{L}_1$ AC transient bounds. We explain how these bounds, which imply arbitrary close tracking of *linear* reference models in the time domain, can be exploited for learning purposes in the iteration domain. We then show how the $\mathcal{L}_1$ AC stability condition relates directly to the robust monotonic convergence conditions of LTI learning laws, and how robust ILC algorithms can be designed in a simple, straightforward manner for different $\mathcal{L}_1$ AC architectures.

The rest of the paper is organized as follows. Section 2 introduces some preliminaries for clarity of exposition. Section 3 gives a brief introduction to $\mathcal{L}_1$ AC and ILC, and presents our proposed method for the state feedback case. Section 4 extends the results to time varying uncertainties in output feedback. Simulation results are given in section 5. Section 6 gives concluding remarks and summarizes our findings. For a streamlined presentation, we give certain intermediate results in Appendix A, proofs of our main results in Appendix B and several auxiliary variables in Appendix C.

2. Notation and Preliminaries

Throughout the paper, we use time and frequency domain representations interchangeably for signals. For example, $f(s)$ denotes the Laplace transform of the signal $f(t)$. We denote systems and matrices with upper case letters. We represent signals and vectors with lower case letters. We use script letters to distinguish linear operators in general from their matrix and transform representations (e.g. $\mathcal{F}$ instead of $F(s)$). We take $\mathbb{R}$ to represent the set of real numbers and $\mathbb{R}^+$ the set of positive real numbers. We choose $\mathbb{C}$ to denote complex numbers. We take $\mathbb{I}$ to be the identity matrix of appropriate size and $\mathcal{I}$ to be the identity operator in the relevant space. We use $\lambda_{max}(.)$ and $\lambda_{min}(.)$ to denote the maximum and minimum eigenvalues of a positive definite matrix, respectively. We take $\|.\|_p$ for $p \in [1, \infty]$ as the standard vector and induced p norm. We use $\mathcal{F}^{-R}$ and $\mathcal{F}^{-L}$ for the right and left inverses of an operator $\mathcal{F}$, respectively; and F^T for the transpose of a matrix F.

In the rest of the section, we collect several definitions and facts from systems theory pertinent to our discussion.

Definition 1. For any $p \in [1, \infty)$, $\mathcal{L}_p^n$ is defined as the space of all piecewise continuous $f : \mathbb{R} \to \mathbb{R}^n$ such that $\|f\|_{\mathcal{L}_p} \triangleq (\int_{-\infty}^{\infty} \|f(t)\|^p dt)^{1/p} < \infty$, where $\|.\|$ is any standard vector norm in $\mathbb{R}^n$. However, it is conventional to use the 2 norm for $\mathcal{L}_2^n$. Similarly, $\mathcal{L}_\infty^n$ is defined as the space of all piecewise continuous $f : \mathbb{R} \to \mathbb{R}^n$ such that $\|f\|_{\mathcal{L}_\infty} \triangleq \sup_{t\in\mathbb{R}} \|f(t)\|_\infty < \infty$.

Definition 2. For any $p \in [1, \infty]$, the extended space $\mathcal{L}_{pe}^n$ is defined as the space of all piecewise continuous causal $f : \mathbb{R} \to \mathbb{R}^n$ such that $\|f_\tau\|_{\mathcal{L}_p} < \infty \ \forall \tau \geq 0$, where f_τ is the truncation of f defined by $f_\tau(t) \triangleq f(t)$ for $0 \leq t \leq \tau$ and $f_\tau(t) \triangleq 0$ for $t > \tau$.

Definition 3. For a given m input n output LTI system $F(s)$ with impulse response $f(t) \in \mathbb{R}^{n\times m}$, the $\mathcal{L}_1$ norm is defined as $\|F(s)\|_{\mathcal{L}_1} \triangleq \max_{k\in 1,2,\ldots,n} \sum_{l=1}^m \|f_{kl}\|_{\mathcal{L}_1}$, where $f_{kl}(t)$ is the entry at the k^{th} row and l^{th} column of $f(t)$.

Definition 4. The $\mathcal{L}_\infty(j\mathbb{R})$ norm of a bounded-input bounded-output (BIBO) stable LTI system $F(s)$ is defined by $\|F(s)\|_\infty \triangleq \sup_{\omega\in\mathbb{R}} \|F(j\omega)\|_2$.[1]

Lemma 1. *Let $F(s)$ be a stable causal LTI system. Then for every bounded input ζ, the output ξ is bounded and we have $\|\xi_\tau\|_{\mathcal{L}_\infty} \leq \|F(s)\|_{\mathcal{L}_1} \|\zeta_\tau\|_{\mathcal{L}_\infty}$ [17, page 273].*

Remark 1. Lemma 1 shows that the $\mathcal{L}_1$ norm of a stable LTI system is essentially its *induced $\mathcal{L}_\infty$ norm*: If $\|F(s)\|_{\mathcal{L}_1} = \sum_{l=1}^m \|f_{kl}\|_{\mathcal{L}_1}$ for some k, the equality can be achieved by taking $u_l(t - \upsilon) = \text{sgn}(f_{kl}(\upsilon))$. This also implies $\|F_1(s)F_2(s)\|_{\mathcal{L}_1} \leq \|F_1(s)\|_{\mathcal{L}_1} \|F_2(s)\|_{\mathcal{L}_1}$ for stable $F_1(s)$, $F_2(s)$. Consequently, an LTI system $F(s)$ is BIBO stable if and only if $\|F(s)\|_{\mathcal{L}_1} < \infty$ [17, page 274], which justifies the use of the $\mathcal{L}_1$ norm in establishing boundedness in $\mathcal{L}_1$ AC algorithms.

Theorem 1. *For a BIBO stable LTI system $F(s)$ the induced $\mathcal{L}_2$ norm is equal to $\|F(s)\|_\infty$ [24, page 101].*

Readers will note that we mainly consider two types of *signal norms*: $\mathcal{L}_\infty$ and $\mathcal{L}_2$. The $\mathcal{L}_\infty$ norm will be used in $\mathcal{L}_1$ AC to establish *boundedness* (lemma 1), while the $\mathcal{L}_2$ norm will be of interest in ILC as a *performance metric*. The following will be used in establishing the relationship between the two for ILC design:

[1] The $\mathcal{L}_\infty(j\mathbb{R})$ norm of a transfer function should not be confused with the $\mathcal{L}_\infty$ norm of a signal in the time domain. For causal $F(s)$, $\|F(s)\|_\infty$ is precisely the $\mathcal{H}_\infty$ norm.

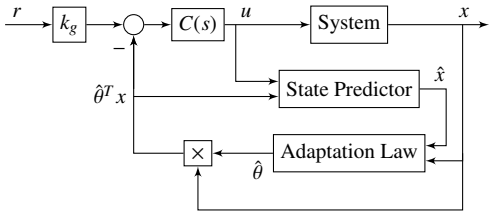

Figure 1: $\mathcal{L}_1$ adaptive control for LTI state feedback with unknown pole locations

Lemma 2. *For a stable causal m input n output LTI system $F(s)$ we have $\|F(s)\|_\infty \leq \sqrt{n}\|F(s)\|_{\mathcal{L}_1}$.*

Remark 2. While lemmas 1 and 2 are given for causal systems, the results are also true in essence for noncausal systems. For example, for a stable noncausal LTI system $F(s)$ with bounded input ζ, the output ξ is bounded and $\|\xi\|_{\mathcal{L}_\infty} \leq \|F(s)\|_{\mathcal{L}_1}\|\zeta\|_{\mathcal{L}_\infty}$. In the rest of the paper, unless otherwise noted, we will assume all systems and signals to be causal.

3. State Feedback

We will start our discussion with the full state feedback $\mathcal{L}_1$ AC architecture (figure 1) for SISO LTI systems with unknown pole locations. This class of systems offers a good introduction to $\mathcal{L}_1$ AC and will show us that the guaranteed transient property holds with the addition of a feedforward signal *in the problem objective*. We will then demonstrate how this property, along with the main stability condition of $\mathcal{L}_1$ AC, can aid us in the design of our learning law. Finally, we will have a brief look at the design trade-offs and argue how $\mathcal{L}_1$ AC and ILC can be combined into a single framework with the unified objectives of high tracking performance, robustness to uncertainties and monotonic transient response in the time and iteration domains.

3.1. $\mathcal{L}_1$ Adaptive Control

$\mathcal{L}_1$ AC is a recently developed model following control methodology [17] with guaranteed transient performance and robustness in the presence of fast adaptation. The central idea of $\mathcal{L}_1$ AC theory lies in the use of the *available bandwidth* of the control channel, imposed by physical hardware [20]. Drawing inspiration from robust and classical control, $\mathcal{L}_1$ AC aims to compensate for uncertainties in a limited range of frequencies, a more "feasible" objective than that of conventional MRAC wherein uncertainties are compensated over the whole spectrum. This approach brings significant advantages over conventional MRAC, the most critical of these being the "decoupling" of estimation and control, realized by the presence of a bandlimited filtering structure at a particular point (which varies depending on the class of systems, see for instance figure 1 for the LTI state feedback with unknown pole locations) in the architecture. As a result of this property, the performance-robustness trade-off of $\mathcal{L}_1$ systems is defined by the bandwidth of the filter as opposed to the rate of adaptation. This trade-off can be addressed with tools from classical and robust control; whereas the adaptation rates can be increased arbitrarily and are limited only by practical concerns such as hardware speed and noise. Consequently, uniform performance bounds on the input and output signals can be enforced by high adaptation rates while still maintaining a relatively high level of robustness [25].

$\mathcal{L}_1$ AC algorithms have been developed for a wide range of classes. In this section, we present the $\mathcal{L}_1$ architecture for SISO LTI systems with unknown constant parameters. To account for changes in system trajectory due to feedforward control, and put the problem into a meaningful format, we augment the original controller [17] with a bounded feedforward signal.

3.1.1. Problem Formulation

We consider the following class of systems

$$\begin{aligned} &\dot{x}(t) = Ax(t) + b(u(t) + \theta^T x(t)), \quad x(0) = x_{in}, \\ &y(t) = c^T x(t), \end{aligned} \tag{1}$$

where $x(t) \in \mathbb{R}^n$ is the measured state vector; $u(t) \in \mathbb{R}$ is the control input; $b, c \in \mathbb{R}^n$ are known constant vectors; $A \in \mathbb{R}^{n\times n}$ is a known constant matrix, with (A, b) controllable; $\theta \in \Theta$ is an unknown constant vector, where Θ is a compact convex set; and $y(t) \in \mathbb{R}$ is the output signal. Without loss of generality, let A be Hurwitz.

Assumption 1. $\Theta = \{\theta \in \mathbb{R}^n : \|\theta\|_\infty \leq \theta_{M_\infty}\}$ for some $\theta_{M_\infty} \in \mathbb{R}^+$.

Remark 3. Assumption 1 will enable us to abuse the relationship of lemma 2 for ILC purposes.

The $\mathcal{L}_1$ AC objective is to track a given reference system in transient and steady state phases.

3.1.2. Closed Loop Reference System

The reference system dynamics are described by $(A, b, c^T, 0)$, the strictly proper BIBO stable transfer function $C(s)$ with DC gain 1 and zero state space initialization, and the unknown parameter θ. $C(s)$ is also subject to the $\mathcal{L}_1$ norm condition

$$\|G(s)\|_{\mathcal{L}_1}\theta_{M_1} < 1, \tag{2}$$

where $G(s) \triangleq H_x(s)(1 - C(s))$, $H_x(s) \triangleq (s\mathbb{I} - A)^{-1}b$; and $\theta_{M_1} \triangleq \max_{\theta\in\Theta} \|\theta\|_1 = n\theta_{M_\infty}$. Let $H(s) \triangleq c^T H_x(s)$. The feedforward augmented closed loop reference system can be defined as

$$\begin{aligned} \dot{x}_{ref}(t) &= Ax_{ref}(t) + b(u_{ref}(t) + \theta^T x_{ref}(t)), \\ y_{ref}(t) &= c^T x_{ref}(t), \\ u_{ref}(s) &= C(s)(k_g r(s) - \theta^T x_{ref}(s)) + u_i(s), \end{aligned} \tag{3}$$

with initial condition $x_{ref}(0) = x_{in}$, where $k_g = 1/H(0)$ is a static precompensator; $r(s)$ is the reference signal; and $u_i(s)$ is a bounded input signal in Laplace notation.

By augmenting the reference system with a feedforward control signal, we reformulate the problem so that the objective is to track certain given dynamics driven by a reference signal *and* a feedforward signal. Since this signal will be synthesized by certain filtering methods, and be used later for performance improvement, we choose not to pass it through $C(s)$. Note that letting $C(s) = 1$ in (3) results in the nominal system given by $(A, b, c^T, 0)$ (i.e. $\theta = 0$) with input $k_g r(t) + u_i(t)$. In that sense, we aim to only partially compensate for uncertainties, within the bandwidth of $C(s)$.

Lemma 3. *If (2) is satisfied, the reference system (3) is bounded-input bounded-state (BIBS) stable.*

Proof. See [17]. The proof follows in the same manner from the boundedness of $u_i(t)$.

Remark 4. Condition (2) ensures that the feedback gain of θ on the system states is small enough for stability (see lemma 7 in Appendix A) since $\|\theta\|_1$ is the $\mathcal{L}_1$ norm of the static LTI system θ^T. In other words, we require the bandwidth of $C(s)$ be high enough for sufficient compensation of uncertainties.

3.1.3. $\mathcal{L}_1$ Adaptive Controller

The $\mathcal{L}_1$ adaptive controller is based on a fast estimation scheme which consists of a state predictor, the bounded feedforward input $u_i(t)$ and the bandlimited filter $C(s)$.

3.1.3.1. State Predictor. The controller relies on the following state predictor

$$\dot{\hat{x}}(t) = A\hat{x}(t) + b(\hat{\theta}^T(t)x(t) + u(t)) - K_{sp}\tilde{x}(t), \tag{4}$$

with initial condition $\hat{x}(0) = x_{in}$, where $\hat{x}(t)$ is the state prediction vector; $\hat{\theta}(t)$ is the estimate of the unknown constant vector θ; $\tilde{x}(t) \triangleq \hat{x}(t) - x(t)$ is the prediction error; and $K_{sp} \in \mathbb{R}^{n\times n}$ can be used to assign faster poles to $(A - K_{sp})$ [26].

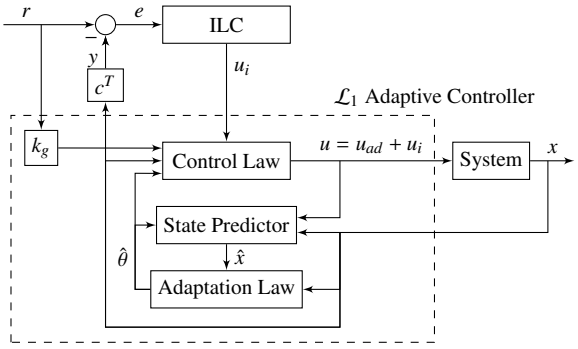

Figure 2: ILC with feedforward augmented $\mathcal{L}_1$ adaptive feedback

3.1.3.2. Adaptation Law. The adaptation law that estimates θ is

$$\dot{\hat{\theta}}(t) = \Gamma \,\mathrm{Proj}(\hat{\theta}(t), -\tilde{x}^T(t)Pbx(t)), \tag{5}$$

with arbitrary initial condition $\hat{\theta}(0) = \hat{\theta}_{in} \in \Theta$, where Proj(.,.) is the projection operator defined in [27], with projection bound $\theta_{M_2} \triangleq \max_{\theta\in\Theta} \|\theta\|_2 = \sqrt{n}\theta_{M_\infty}$; $\Gamma > 0$ is the adaptation rate; and $P = P^T > 0$ is the solution to the algebraic Lyapunov equation $A^T P + PA = -Z$, with arbitrary $Z = Z^T > 0$. The projection operator ensures the boundedness of $\hat{\theta}(t)$ by definition. This property is used extensively in the analysis of $\mathcal{L}_1$ schemes.

3.1.3.3. Control Law. The control input is defined as

$$\begin{aligned} u(t) &= u_{ad}(t) + u_i(t), \\ u_{ad}(s) &\triangleq C(s)(k_g r(s) - \hat{\eta}(s)), \end{aligned} \tag{6}$$

where $u_{ad}(t)$ and $u_i(t)$ are the feedback and feedforward signals, respectively; and $\hat{\eta}(s)$ is the Laplace transform of $\hat{\theta}^T(t)x(t)$. Inclusion of the feedforward signal in the control input leads to the augmentation of the state predictor (see figure 2). Hence, the controller generates the proper adaptive signal $u_{ad}(t)$ to track (3).

3.1.4. Transient Performance

The controller ensures transient and steady-state behavior in the input and output channels with respect to the $\mathcal{L}_1$ reference system, as stated in the theorem below.

Theorem 2. *For system (1) with the controller defined according to (4), (5) and (6), subject to the $\mathcal{L}_1$ norm condition (2); and its corresponding reference system (3), we have*

$$\begin{aligned} \|x_{ref} - x\|_{\mathcal{L}_\infty} &\leq \tfrac{\chi_1}{\sqrt{\Gamma}}, \ \lim_{t\to\infty}(x_{ref}(t) - x(t)) = 0, \\ \|u_{ref} - u\|_{\mathcal{L}_\infty} &\leq \tfrac{\chi_2}{\sqrt{\Gamma}}, \ \lim_{t\to\infty}(u_{ref}(t) - u(t)) = 0, \end{aligned} \tag{7}$$

where $\chi_1, \chi_2 \in \mathbb{R}$ are defined in [17].

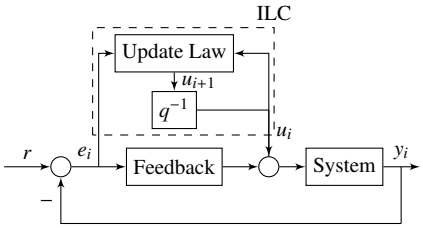

Figure 3: Parallel ILC Scheme with the forward trial shift operator q and update law $u_{i+1} = qu_i = f(u_i, e_i)$

Proof. See [17]. The proof is the same since $x_{ref}(t) - x(t)$ and $u_{ref}(t) - u(t)$ do not change with the choice of $u_i(t)$.

Theorem 2 implies that while itself being nonlinear, the $\mathcal{L}_1$ adaptive controller can track the linear reference model arbitrarily closely as Γ is increased. Since ILC uses information from the input and output channels, this property enables the use of the reference model in designing the ILC update law. Moreover, the reference system can be made arbitrarily close to the *design system*, at the expense of reduced robustness, by increasing the bandwidth of $C(s)$. For further details, we refer the readers to [17].

3.2. Iterative Learning Control

ILC architectures can be broadly classified as parallel or series in terms of their relation to feedback control loops. The parallel architecture, which we use in our controller (compare the $\mathcal{L}_1$ AC formulation in section 3.1.2 with figure 3), divides the input signal into feedback and feedforward components. In this approach, the feedforward signal for the next iteration is synthesized by processing the error and the feedforward input at the current iteration.

ILC design methods are numerous and include frequency domain, plant inversion, and optimization techniques. While frequency domain methods only approximate the system due to finite trial duration, they offer simplicity, flexibility and tunability as in classical control. For these reasons, we will be adopting frequency domain methods to design our learning law. Further details on ILC can be found in [1].

3.2.1. Update Law

A common first order frequency domain ILC algorithm, which we will employ, is the Q filter and learning function approach:

$$u_{i+1}(s) = Q(s)(u_i(s) + L(s)e_i(s)). \tag{8}$$

In (8), $u_i(s)$ is the ILC input; $Q(s)$ is the Q filter; $L(s)$ is the learning function; $e_i(s)$ is the reference tracking error; and i is the iteration index. In this approach, $L(s)$ is used to maximize learning, while $Q(s)$ limits the bandwidth for robustness and other practical purposes at the expense of performance. Asymptotic stability and monotonic convergence of the algorithm is given by the following well known theorem:

Theorem 3. *The ILC system, defined by the update law (8) acting on a stable SISO LTI system $F(s)$, is monotonically convergent if $\|Q(s)(\mathbb{I} - L(s)F(s))\|_\infty \leq \mu_F < 1$ for some μ_F. That is, $\|u_\infty - u_{i+1}\|_{\mathcal{L}_2} \leq \mu_F \|u_\infty - u_i\|_{\mathcal{L}_2}$, $i = 0, 1, \ldots$, where $u_\infty(t)$ is the converged input.*

Remark 5. As causality is not a constraint in ILC, the readers might ask if the condition is valid for noncausal $Q(s)$ and $L(s)$. The answer is yes, since the theorem is proven by defining a contraction in the input space $\mathcal{L}_2$ by aid of theorem 1. Readers interested in the use of noncausal LTI operators in ILC can refer to [28].

3.2.2. Monotonic Convergence and Robustness

Recall the guaranteed transient property of the adaptive system as stated in (7). For the design of the update law, we will assume Γ is sufficiently high, and consequently that $x(t) = x_{ref}(t)$. Nevertheless, since the $\mathcal{L}_1$ controller aims to compensate for uncertainties within the bandwidth of $C(s)$, parametric uncertainties will still exist. The closed loop system can be described as

$$y_i(s) = \bar{H}(s)u_i(s) + \bar{H}(s)C(s)k_g r(s) + c^T(\mathbb{I} - G(s)\theta^T)^{-1}x_{nr}(s),$$

where $\bar{H}(s) \triangleq c^T(\mathbb{I} - G(s)\theta^T)^{-1}H_x(s) = H(s)/1 - \theta^T G(s)$ by lemma 8 in Appendix A; and $x_{nr}(s) \triangleq (s\mathbb{I} - A)^{-1}x_{in}$.

While theorem 3 ensures monotonic convergence in the $\mathcal{L}_2$ space for a nominal system, it does not guarantee the same under uncertainty. We now state our main result which shows that for the $\mathcal{L}_1$-ILC scheme, robust monotonic convergence can be guaranteed in a very simple way.

Theorem 4. *The ILC system with the update law (8) defined over $\bar{H}(s)$ subject to (2), is monotonically convergent with rate $\mu \in [0, 1)$ $\forall \theta \in \Theta$ if*

$$\kappa \leq \frac{\mu - |Q(j\omega)||1 - L(j\omega)H(j\omega)|}{|Q(j\omega)||L(j\omega)||H(j\omega)|}, \tag{9}$$

$\forall \omega \in \mathbb{R}$, where

$$\kappa \triangleq \frac{\theta_{M_2}\|G(s)\|_\infty}{1 - \theta_{M_2}\|G(s)\|_\infty}. \tag{10}$$

Remark 6. Theorem 4 is a natural result of theorem 6 of [1] when the uncompensated uncertainty is written in multiplicative uncertainty form. See Appendix B for the details.

Theorem 3 states that the nominal system can be rendered monotonically convergent by defining a contraction mapping in the input space. Theorem 4, on the other hand, directly extends monotonic convergence to the $\mathcal{L}_1$-AC scheme by making sure that the update law defines a contraction $\forall\theta \in \Theta$. More specifically, (9) implies $\max_{\theta\in\Theta} \|Q(s)(1 - L(s)\bar{H}(s))\|_\infty \leq \bar{\mu} < 1$ for some $\bar{\mu}$. This condition follows elegantly from the $\mathcal{L}_1$ norm condition which ensures that the plant uncertainty $(1 - \theta^T G(s))^{-1}$ exists and is BIBO stable.

3.3. Design Trade-Offs

For a better understanding of the combined $\mathcal{L}_1$-ILC scheme, we will have a look at the design trade-offs. We first define $\Lambda(s) \triangleq (1 - \theta^T G(s))^{-1}$. The inequalities below follow directly from the definitions of $\Lambda(s)$ and $\bar{\mu}$:

$$|\Lambda(j\omega)| \geq \frac{1}{|1 - \theta^T H_x(j\omega)| + |C(j\omega)||\theta^T H_x(j\omega)|},$$

$$\frac{\bar{\mu}}{|Q(j\omega)|} \geq |1 - |L(j\omega)H(j\omega)\Lambda(j\omega)||.$$

It follows that

$$|L(j\omega)||H(j\omega)| \leq \left(\frac{\bar{\mu}}{|Q(j\omega)|} + 1\right) \times (|1 - \theta^T H_x(j\omega)| + |C(j\omega)||\theta^T H_x(j\omega)|). \quad (11)$$

Recall that $C(s)$ and $Q(s)$ describe the performance-robustness trade-offs in their respective domains. Thus, generally speaking, we can conclude the following:

1. Increasing the bandwidth of $C(s)$ decreases the minimum $\bar{\mu}$ that satisfies (11), i.e. faster convergence. Indirectly, a higher bandwidth also results in better iteration domain robustness since $\bar{\mu}$ becomes bounded further away from 1, thereby leaving the possibility of higher gain Q filters for enhanced performance: As the bandwidth of $C(s)$ increases, κ, as defined in (10), decreases since $\|G(s)\|_\infty \leq \|H_x(s)\|_\infty \|1 - C(s)\|_\infty$. As a result, the designer can tune $Q(s)$ to increase its bandwidth and minimize the converged error.
2. Decreasing the bandwidth of $Q(s)$ decreases the minimum $\bar{\mu}$ that would satisfy (11), which signifies increased iteration domain robustness. This further implies that one can use a lower gain $C(s)$ for a feedback system with better stability margins: Because $Q(s)$ has a lower gain, there exists a higher value of κ satisfying (9) for the initial value of $\bar{\mu}$.

It thus makes sense to summarize the design trade-offs for the combined $\mathcal{L}_1$-ILC scheme as that of performance versus robustness. Intuitively, this is to be expected as increasing the passband of $C(s)$ decreases uncertainty $\Lambda(s) = (1 - \theta^T H(s)(1 - C(s)))^{-1}$, which is the desired result from an ILC perspective. For further insight into the controller, we refer the readers to [22] where we provide extensive simulations showcasing decreasing effects of uncertainty with increasing feedback bandwidth, and similar performance for all uncertainties and bandwidths such that the closed loop system remains stable.

3.4. Practical Considerations and Design Guidelines

The level of detail surrounding the previous sections may leave the impression that the design of the combined $\mathcal{L}_1$-ILC algorithm is highly complicated. In reality, despite the algebraic intensity of the analysis, the adaptive and learning controllers rely on fundamental ideas of classical and robust control. Hence, in this section we will explore how the controller can be designed in a relatively straightforward way using these ideas. The trade-offs given in section 3.3 will be helpful towards that end.

The obvious starting point of this procedure is the design of the $\mathcal{L}_1$ adaptive feedback controller. Readers would note that the main design decisions of $\mathcal{L}_1$ AC are the bandwidth of the feedback filter $C(s)$ and the magnitude of the adaptation rate Γ. At this point we would like to direct the readers' attention to theorem 2 and remind that the theoretical model tracking error of the feedback system can be set *arbitrarily low*. Therefore, the design of the filter and selection of the adaptation rate are *decoupled*. As we have mentioned in section 3.3, $C(s)$ describes the performance-robustness trade-off in the time domain; i.e. a higher closed loop bandwidth results in decreased robustness margins and vice versa. Thus, the natural question that follows is if the $\mathcal{L}_1$ norm condition can be satisfied. The lemma below illustrates how this is indeed always possible:

Lemma 4. *Let* $F(s) = \frac{\prod_{k=1}^{m}(s+z_k)}{\prod_{k=1}^{n}(s+p_k)}$ *be strictly proper and causal. Assume there exists* $\psi \in (\pi/2, \pi]$ *such that* $arg(p_k) \in [\psi, 2\pi - \psi]$, $k = 1, 2, \ldots, n$. *Then, as* $\min_{k=1,2,\ldots,n} |p_k| \to \infty$, $\|F(s)\|_{\mathcal{L}_1} \to 0$.

Let us assume the filter $C(s)$ is chosen in the form of $1 - s^n/(s^n + a_{n-1}s^{n-1} + \cdots + a_0)$, which guarantees that the

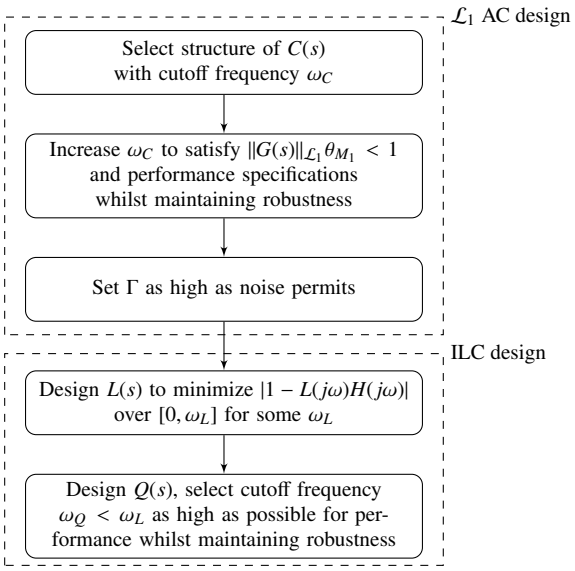

Figure 4: Design flowchart of the $\mathcal{L}_1$-ILC scheme

DC gain of $C(s)$ is 1 and that the numerator of $1 - C(s)$ is constant regardless of the choice of poles. Now, we have

$$\|G(s)\|_{\mathcal{L}_1} \leq \|\frac{s^{n-1}}{s^n + a_{n-1}s^{n-1} + \cdots + a_0}\|_{\mathcal{L}_1}\|sH_x(s)\|_{\mathcal{L}_1}.$$

The above lemma then implies that $\|G(s)\|_{\mathcal{L}_1}$ can be rendered arbitrarily small to satisfy the $\mathcal{L}_1$ stability condition (2) by increasing the bandwidth of $C(s)$ since $\|sH_x(s)\|_{\mathcal{L}_1} \in \mathbb{R}$ from the stability assumption and the strict properness of $H_x(s)$. Observe that an obvious choice for $C(s)$ is $\omega_C/(s + \omega_C)$ and note that for a given $C(s)$ the $\mathcal{L}_1$ adaptive controller has guaranteed (bounded away from 0) robustness margins [17]. Hence, after $C(s)$ is designed, the adaptation rate should be set as high as possible, while taking into consideration that large values of Γ might amplify noise and hinder closed loop performance.

Once the adaptive control design is finalized, the learning function can be designed on the nominal system (i.e. $\theta = 0$) via the well known Nyquist tuning method [1]. A good rule of thumb to minimize the converged error is to set $|1 - L(j\omega)H(j\omega)|$ small within a large bandwidth since

$$e_\infty(s) = \frac{1 - Q(s)}{1 - Q(s)(1 - L(s)H(s))}e_{fb}(s),$$

for $\theta = 0$, where $e_{fb}(s)$ is the feedback error without any feedforward input. The Q filter can then be used to limit this bandwidth so that the learning controller is robust against unmodeled high frequency dynamics, noise, and the uncompensated parametric uncertainty $\Lambda(s)$ as per theorem 4.

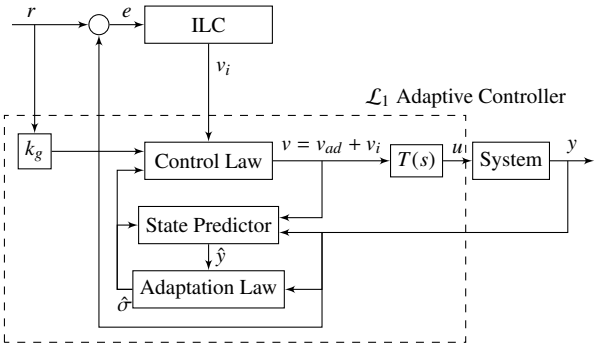

Figure 5: ILC with feedforward augmented $\mathcal{L}_1$ adaptive output feedback

In light of these observations, the design procedure has been summarized in figure 4. We remind the readers that while higher values of ω_C and ω_Q signify high closed loop and learning performance, this comes at the expense of *reduced stability margins*.

4. Output Feedback

The results of section 3 show us that by a slight modification of the $\mathcal{L}_1$ AC formulation, we can preserve the guaranteed transient property of the feedback controller. By doing so, we make sure that the $\mathcal{L}_1$ controller uses information from the feedforward input and keeps the plant sensitivity close to the nominal case for performance improvement through learning. In this section we extend the results of section 3 to the output feedback case with time varying unknown feedback gains and input disturbances. While the structure of the $\mathcal{L}_1$ controller is slightly different and less intuitive, we see that the results are similar from an ILC standpoint. We follow the same procedure of defining the feedforward augmented adaptive controller, and designing an iterative update law under the assumption of high adaptation gain. Unless, explicitly stated, our assumptions and definitions from section 3 will continue to hold.

4.1. $\mathcal{L}_1$ Adaptive Control

We present the $\mathcal{L}_1$ adaptive output feedback control architecture (figure 5) for SISO linear systems with unknown time varying parameters and disturbances. Our main assumption is that the nominal system is minimum phase and of relative degree 1. The $\mathcal{L}_1$ controller for this class of systems considers an equivalent, *virtual system*

with a virtual adaptive control input [29]. This virtual control signal is passed through a BIBO stable filter to synthesize the actual control input. Hence, we augment this virtual adaptive system with a virtual feedforward signal for learning purposes.

For completeness, we list some variables that are used in the analysis of the original controller [29] in Appendix C. We include some minor changes to account for the addition of an additional input in the adaptive controller.

4.1.1. Problem Formulation

Consider the class of systems

$$\begin{aligned} \dot{x}(t) &= Ax(t) + b(u(t) + \theta^T(t)x(t) + \sigma(t)), \\ y(t) &= c^T x(t), \end{aligned} \tag{12}$$

with initial condition $x(0) = x_{in}$, where $x(t)$ is the *unmeasured* state vector; and $\sigma(t) \in \mathbb{R}$, $|\sigma(t)| \leq \Delta$ for some $\Delta \in \mathbb{R}^+$, is the time varying bounded disturbance.

Assumption 2. $H(s)$ is minimum phase with relative degree 1.

Assumption 3. $\theta(t)$ and $\sigma(t)$ are continuously differentiable with uniformly bounded derivatives; i.e. there exist $d_\theta, d_\sigma \in \mathbb{R}^+$ such that $\|\dot{\theta}(t)\|_2 \leq d_\theta$ and $|\dot{\sigma}(t)| \leq d_\sigma$.

The $\mathcal{L}_1$ AC objective is to track a given reference system in transient and steady state phases by using only output feedback.

4.1.2. System Transformation

In this section, we restate definitions and a lemma from [29] which will define our virtual system. Let

$$\begin{aligned} H_n(s) &\triangleq b_1 s^{n-1} + b_2 s^{n-2} + \cdots + b_n, \\ H_d(s) &\triangleq s^n + a_1 s^{n-1} + \cdots + a_n, \end{aligned}$$

where $a_k, b_k \in \mathbb{R}$ for $k = 1, 2, \ldots, n$ so that we have $H(s) = H_n(s)/H_d(s)$. Further let $A_T \in \mathbb{R}^{n \times n}$ such that the following equality holds:

$$H_x(s) = \frac{A_T \begin{bmatrix} 1 & s & \ldots & s^{n-1} \end{bmatrix}^T}{H_d(s)}.$$

Note that $H(s)$ is stable, minimum phase, and with relative degree 1 by assumption. Hence $H_n(s)$ and $H_d(s)$ are stable polynomials of order n and $n-1$, respectively ($b_1 \neq 0$). Define

$$A_m \triangleq \begin{bmatrix} 0 & 1 & 0 & \ldots & 0 \\ 0 & 0 & 1 & \ldots & 0 \\ \vdots & \vdots & \vdots & \ddots & \vdots \\ 0 & 0 & 0 & \ldots & 1 \\ -a_n & -a_{n-1} & -a_{n-2} & \ldots & -a_1 \end{bmatrix},$$
$$b_m \triangleq \begin{bmatrix} 0 & \ldots & 0 & 1 \end{bmatrix}^T.$$

Since A_m is Hurwitz, for any $Z_m = Z_m^T > 0$ there exists $P_m = P_m^T > 0$ that solves $A_m^T P_m + P_m A_m = -Z_m$. Let $c_m \triangleq P_m b_m$. By the Kalman-Yakubovich-Popov lemma [30], $H_m(s) \triangleq c_m^T (s\mathbb{I} - A_m)^{-1} b_m = H_p(s)/H_d(s)$ is strictly positive real (SPR). For a given signal $v(s)$, let

$$u(s) = T(s)v(s), \tag{13}$$

where $T(s) \triangleq H_p(s)/H_n(s)$ with zero state space initialization. Further let $w_x(s)$ be the output of the following system $\mathcal{W}$:

$$\begin{aligned} w_x(s) &= T^{-1}(s) w_1(s), \\ w_1(t) &= \theta^T(t) w_2(t), \\ w_2(s) &= T(s) A_T x(s). \end{aligned} \tag{14}$$

Lemma 5. *Given $v(t)$, $\theta(t)$, and $\sigma(t)$, there exists a signal $\sigma_m(t)$, $|\sigma_m(t)| \leq \Delta_m$ and $|\dot{\sigma}_m(t)| \leq d_{\sigma_m}$ for some $\Delta_m, d_{\sigma_m} \in \mathbb{R}^+$, such that the output $y(t)$ of (12) with input $u(t)$ synthesized according to (13) is equal to the output $y_m(t)$ of the following system:*

$$\begin{aligned} \dot{x}_m(t) &= A_m x(t) + b_m(v(t) + w_{x_m}(t) + \sigma_m(t)), \\ y_m(t) &= c_m^T x_m(t), \quad x_m(0) = \hat{x}_{in}, \end{aligned} \tag{15}$$

where $w_{x_m}(t)$ is the output of (14) with the input $x(t)$ replaced by $x_m(t)$ and $\hat{x}_{in}$ is any point such that we have $c_m^T \hat{x}_{in} = c_m^T x_{in}$ [29].

Since the above lemma states equivalence of the outputs for arbitrary $v(t)$, we can proceed with (15) as the actual system with proper modification of $v(t)$.

4.1.3. Closed Loop Reference System

With proper modification of $v_{ref}(t)$, the augmented closed loop reference system can be defined as

$$\begin{aligned} \dot{x}_{ref}(t) &= A_m x_{ref}(t) + b_m(v_{ref}(t) + w_{x_{ref}}(t) + \sigma_m(t)), \\ v_{ref}(s) &= C(s)\bar{r}_{ref}(s) + v_i(s), \\ y_{ref}(t) &= c_m^T x_{ref}(t), \end{aligned} \tag{16}$$

with initial condition $x_{ref}(0) = \hat{x}_{in}$, where $w_{x_{ref}}(t)$ is the output of $\mathcal{W}$ with the input $x(t)$ replaced by $x_{ref}(t)$; $\bar{r}_{ref}(t) \triangleq k_g r(t) - w_{x_{ref}}(t) - \sigma_m(t)$ with $k_g \triangleq 1/H_m(0)$; $v_i(t)$ is an arbitrary bounded signal; and $C(s)$ is subject to the $\mathcal{L}_1$ norm condition

$$\|G_m(s)\|_{\mathcal{L}_1} M < 1, \tag{17}$$

with $G_m(s) \triangleq H_{xm}(s)(1 - C(s))$, $H_{xm}(s) \triangleq (s\mathbb{I} - A_m)^{-1} b_m$; and $M \triangleq \|T^{-1}(s)\|_{\mathcal{L}_1} \theta_{M_1} \|T(s) A_T\|_{\mathcal{L}_1}$.

Lemma 6. *If (17) is satisfied, the reference system (16) is BIBS stable.*

Proof. See [29]. The proof follows in the same manner from the boundedness of $v_i(t)$.

Corollary 1. *For $\theta(t) = \theta$, the reference system (16) is BIBS stable if*

$$\|G_m(s)\|_{\mathcal{L}_1}\theta_{M_1}\|A_T\|_{\mathcal{L}_1} < 1. \tag{18}$$

Proof. The proof is omitted and is similar to the proof of lemma 3.

4.1.4. $\mathcal{L}_1$ Adaptive Controller

The $\mathcal{L}_1$ adaptive controller for the virtual system is similar to that of the state feedback case, with the exception that we have a single adaptive law that estimates the combined effects of $w_{x_m}(t)$ and $\sigma_m(t)$.

4.1.4.1. State Predictor. The controller has the following state predictor

$$\begin{aligned}\dot{\hat{x}}(t) &= A_m\hat{x}(t) + b_m(v(t) + \hat{\sigma}(t)),\\ \hat{y}(t) &= c_m^T\hat{x}(t),\end{aligned} \tag{19}$$

with initial condition $\hat{x}(0) = \hat{x}_{in}$, where $\hat{y}(t)$ is the output prediction signal; and $\hat{\sigma}(t)$ is the output of the adaptation law below.

4.1.4.2. Adaptation Law. The adaptation law is given as

$$\dot{\hat{\sigma}}(t) = \Gamma_c\,\mathrm{Proj}(\hat{\sigma}(t), -\tilde{y}(t)), \quad \hat{\sigma}(0) = 0, \tag{20}$$

where $\tilde{y}(t) \triangleq \hat{y}(t) - y_m(t) = \hat{y}(t) - y(t)$ is the output prediction error; the projection is defined with the bound $\bar{\Delta}$ given in Appendix C; and Γ_c is the adaptation rate subject to

$$\Gamma_c > \max\left\{\frac{\alpha\beta_3}{(\alpha-1)^2\beta_4\lambda_{min}(P_m)}, \frac{\alpha\beta_4}{\lambda_{min}(P_m)\bar{\gamma}^2}\right\},$$

with $\alpha > 1$ arbitrary and $\beta_3, \beta_4, \bar{\gamma}$ defined in Appendix C.

4.1.4.3. Control Law. The control law is given by

$$\begin{aligned}v(t) &= v_{ad}(t) + v_i(t),\\ v_{ad}(t) &\triangleq C(s)(k_g r(s) - \hat{\sigma}(s)),\end{aligned} \tag{21}$$

where $v_{ad}(t)$ and $v_i(t)$ are the feedback and feedforward signals, respectively.

4.1.5. Transient Performance

The guaranteed transient property of the controller is given by the following theorem.

Theorem 5. *For system (15) with the controller defined according to (19), (20) and (21), subject to the $\mathcal{L}_1$ norm condition (17); and its corresponding reference system (16), we have*

$$\begin{aligned}&\|y_{ref} - y_m\|_{\mathcal{L}_\infty} = \|y_{ref} - y\|_{\mathcal{L}_\infty} \le \tfrac{\gamma_1}{\sqrt{\Gamma_c}},\\ &\|v_{ref} - v\|_{\mathcal{L}_\infty} \le \tfrac{\gamma_2}{\sqrt{\Gamma_c}}.\end{aligned}$$

Proof. See [29]. The proof follows the same structure with the redefinitions in Appendix C.

4.2. Iterative Learning Control

Having proved that the transient property holds with our additional feedforward signal, we are ready to design a learning law on the adaptive system for performance improvement. The recipe is the same as before and we will be using the nominal system to check robust monotonic convergence by bounding the system uncertainty.

4.2.1. Update Law

We use the Q filter and learning function approach as per section 3 for simplicity and consistency with the state feedback case:

$$v_{i+1}(s) = Q(s)(v_i(s) + L(s)e_i(s)). \tag{22}$$

Note that since we consider (16) for design and analysis, we define the update law on the virtual control $v(s)$ as opposed to the actual control $u(s)$ (see figure 5).

4.2.2. Monotonic Convergence and Robustness

We will design the learning controller under the same assumption as in the state feedback case; $x_m(t) = x_{ref}(t)$. We first analyze the case of constant feedback gain, i.e. $\theta(t) = \theta$. The closed loop reference system can then be described as

$$\begin{aligned}x_{m_i}(s) = H_{xm}(s)v_i(s) + H_{xm}(s)C(s)k_g r(s) +\\ G_m(s)\theta^T A_T x_{m_i}(s) + G_m(s)\sigma_m(s) + x_{nr}(s),\end{aligned} \tag{23}$$

where $x_{nr}(s) \triangleq (s\mathbb{I} - A_m)^{-1}\hat{x}_{in}$, which leads to

$$\begin{aligned}&y_{m_i}(s) = \bar{H}_m(s)v_i(s) + \bar{H}_m(s)C(s)k_g r(s) +\\ &\bar{H}_m(s)(1 - C(s))\sigma_m(s) + c_m^T(\mathbb{I} - G_m(s)\theta^T A_T)^{-1}x_{nr}(s),\end{aligned}$$

where $\bar{H}_m(s) \triangleq c_m^T(\mathbb{I} - G_m(s)\theta^T A_T)^{-1}H_{xm}(s)$. The following extends the result of theorem 4 to the output feedback case. Note that the condition is identical in structure to condition to (9).

Theorem 6. *The ILC system with the update law (22) defined over $\bar{H}_m(s)$ subject to (17) or (18), is monotonically convergent with rate $\mu_m \in [0,1)\ \forall \theta \in \Theta$ if*

$$\kappa_m \leq \frac{\mu_m - |Q(j\omega)||1 - L(j\omega)H_m(j\omega)|}{|Q(j\omega)||L(j\omega)||H_m(j\omega)|},$$

$\forall \omega \in \mathbb{R}$, *where*

$$\kappa_m \triangleq \frac{\theta_{M_2}\|A_T G_m(s)\|_\infty}{1 - \theta_{M_2}\|A_T G_m(s)\|_\infty}.$$

Proof. The proof follows the same steps as that of theorem 4 and is omitted.

We note that in both the state and output feedback cases, theorems 4 and 6 show that the contraction mapping condition can be guaranteed for all uncertainties by well defined relationships that result from the $\mathcal{L}_1$ norm condition and bounds on the induced norms of the uncertainties. Therefore, we can extend the convergence conditions to time varying feedback in a similar fashion. To that end, we will rewrite the plant dynamics in operator form. Observe that in (23), the mapping $\theta^T A_T$ is in essence the system $\mathcal{W}$ that maps x_i to w_{x_i} for the special case of constant θ. Therefore, the plant dynamics can be rewritten in more general form as

$$x_{m_i} = \mathcal{H}_{xm} v_i + \mathcal{H}_{xm} C k_g r + \mathcal{G}_m \mathcal{W} x_{m_i} + \mathcal{G}_m \sigma_m + x_{nr}, \quad (24)$$

where $\mathcal{H}_{xm}$, C and $\mathcal{G}_m$ are $H_{xm}(s)$, $C(s)$ and $G_m(s)$ in operator notation, respectively. Note that the dynamics are the same with the exception of $\mathcal{W}$ being a linear time varying map, which prevents us from further simplification in the s domain. Regardless, we see after some manipulations that the $\mathcal{L}_2$ gain of the uncertainty and therefore the robust monotonic convergence condition is very similar.

Theorem 7. *The ILC system with the update law (22) defined over (24) subject to (17), is monotonically convergent with rate $\mu_{m_{tv}} \in [0,1)\ \forall \theta(t) \in \Theta$ if*

$$\kappa_{m_{tv}} \leq \frac{\mu_{m_{tv}} - \|Q(s)(1 - L(s)H_m(s))\|_\infty}{\|Q(s)L(s)H_m(s)\|_\infty}, \quad (25)$$

where

$$\kappa_{m_{tv}} \triangleq \frac{M_2\|T(s)A_T H_{xm}(s)\|_\infty \|1 - C(s)\|_\infty}{1 - M_2\|T(s)A_T G_m(s)\|_\infty},$$

with $M_2 \triangleq \|T^{-1}(s)\|_\infty \theta_{M_2}$.

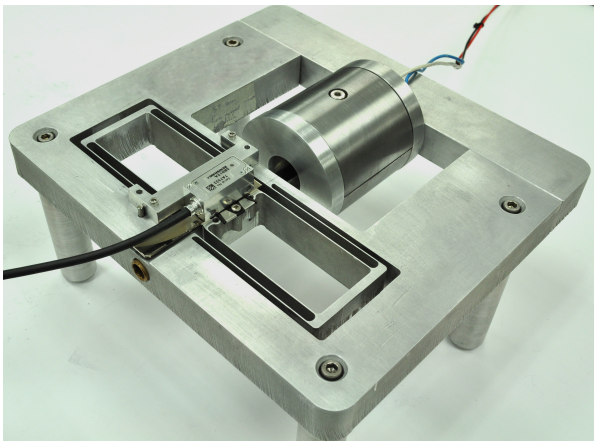

Figure 6: Single axis flexure bearing based nanopositioner with moving magnet actuator [31]

Due to the time varying nature of the feedback uncertainty, theorem 7 is naturally more conservative than theorem 6. Algebraically, this is attested to the fact that we cannot simplify $\mathcal{W}$ and commute SISO operators as in matrix notation. Physically, we can interpret this as the effect of time varying parameters being much less predictable than that of constant parameters. Nevertheless, due to the condition being conservative, we might see in practice that the actual performance of ILC is much better than expected. We would also like to add that the design trade-offs of the output feedback $\mathcal{L}_1$-ILC scheme can be evaluated straightforwardly much as in section 3.3. We omit these for the sake of brevity.

5. Simulations

To illustrate the benefits of our proposed method, we will consider an $\mathcal{L}_1$ AC based ILC design on a model of the flexure bearing based nanopositioner shown in Figure 6 [31]. In [31], the authors consider the following output compensator

$$D(s) = \frac{1.57 \times 10^4 (s + 141.5)}{s(s + 4000)} \times \frac{(s^2 + 159.5s + 5.01 \times 10^4)}{(s^2 + 6700s + 1.92 \times 10^7)},$$

designed on the open loop transfer function from the actuator input, identified as

$$P(s) = \frac{1.28 \times 10^{10}(s^2 + 5.63s + 3.34 \times 10^5)}{(s + 333.1)(s^2 + 150.50s + 3.31 \times 10^4)} \times \frac{1}{(s^2 + 12.43s + 3.87 \times 10^5)},$$

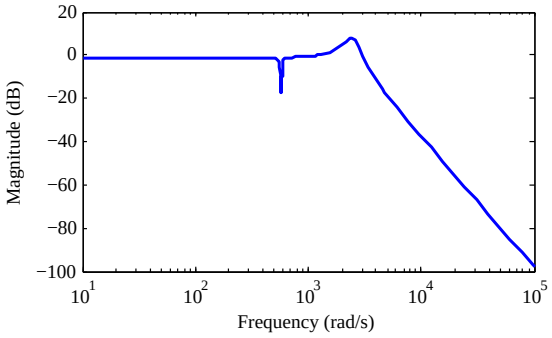

Figure 7: Bode magnitude plot of the closed loop complementary sensitivity function $T_p(s)$ of the flexure bearing based nanopositioner

which results in the closed loop complementary sensitivity function $T_P(s) \triangleq D(s)P(s)/(1 + D(s)P(s))$ by unity gain feedback (Figure 7). Since $P(s)$ was obtained through system identification, we do a balanced realization to come up with the system matrices $\bar{A}$, b, and c such that $P(s) = c^T(s\mathbb{I} - \bar{A})^{-1}b$. To simulate an uncertainty in the pole locations, we assume a time varying $\theta(t)$, subject to $\theta_{M_\infty} = 1$, with a bounded derivative.

We will be considering two feedback based learning schemes to compare on the plant $(\bar{A}, b, c^T, 0)$ with the uncertain feedback gain $\theta(t)$. The control objective is to minimize the tracking error for dynamic references within 10 rad/s, regardless of the level of uncertainty imposed by $\theta(t)$. We would like to see similar learning performances and converged tracking errors for every $\theta(t)$. Furthermore, we expect that performance degradations due to abrupt changes in $\theta(t)$ to be low, and can be compensated within a few iterations.

5.1. LTI Output Feedback based ILC (LTI-ILC) Design

We consider the output compensator of [31] and take the control law as $u_{LTI_i}(s) = D(s)((r(s) + u_i(s)) - y_i(s))$, where $u_{LTI_i}(s)$ is the control input and $u_i(s)$ is the feedforward learning signal. Note that this results in the dynamics given by $y_i(s) = T_p(s)u_i(s) + T_p(s)r(s)$, which is similar to the iteration domain dynamics in section 3.2.2 under zero initial conditions and $\theta(t) = 0$.

The signal $u_i(s)$ is given by the update law (8), with

$$Q(s) = \frac{250}{s + 250}, \quad L(s) = \frac{5000}{s + 5000}.$$

The filter $L(s)$ is designed to approximate the inverse of $T_p(s)$ and to keep $|1 - L(j\omega)T_p(j\omega)|$ small over a large bandwidth, while $Q(s)$ is chosen to maintain stability whilst having a sufficiently high bandwidth. More specifically, the cutoff frequency of $L(s)$ was chosen to be higher than that of $T_p(s)$ for ample learning, while $Q(s)$ was chosen to be more than a decade faster than the desired tracking bandwidth of 10 rad/s. The signal $u_i(s) + L(s)e_i(s)$ is passed through $Q(s)$ twice via time reversal to emulate zero phase filtering in continuous time and eliminate the phase lag in the ILC signal. Note that the gain of this process is $|Q(j\omega)|^2$ due to double filtering.

5.2. State Feedback $\mathcal{L}_1$ AC based ILC Design

For the proposed $\mathcal{L}_1$-ILC scheme, we employ a static feedback k_{fb} such that the closed loop response given by $(A, b, c, 0)$, where $A = \bar{A} - bk_{fb}^T$, is similar to $T_p(s)$ under zero uncertainty (i.e. $\theta(t) = 0$). We select the desired pole locations as the poles of the reduced order (5^{th}) approximation to $T_p(s)$ to yield near identical step responses for $k_g H(s) = k_g c^T(s\mathbb{I} - A)^{-1}b$ and $T_p(s)$.

In the $\mathcal{L}_1$ AC design, we consider a 3^{rd} order filter and take $C(s) = 1 - s^3/(s + \omega_C)^3$ to better attenuate the effects of $\theta(t)$, which satisfies (2) for $\omega_C \geq 2600$. To avoid an excessive bandwidth, we choose $\omega_C = 3000$, and also note that condition (2) can be satisfied by a lower bandwidth through careful selection of the desired pole locations, since the lightly damped poles of $T_p(s)$ (and consequently $H(s)$ by virtue of the selected poles) manifest as high gain feedback through $\theta(t)$ in terms of the $\mathcal{L}_1$ norm condition. We consider a noisy measurement scenario wherein each state is corrupted by Gaussian white noise with variance 3.16×10^{-8}, which results in an output noise variance of 1.96×10^{-5}. To limit noise amplification, we take the adaptive gain Γ to be 1×10^6. For the state predictor, we select $K_{sp} = 0$ for simplicity.

For the ILC update law, we choose

$$Q(s) = \frac{250}{s + 250}, \quad L(s) = k_g\frac{5000}{s + 5000},$$

which result in a similar learning performance to that of the output feedback based design. As with the LTI-ILC scheme, we filter $u_i(s) + L(s)e_i(s)$ through $Q(s)$ twice to eliminate phase lag.

5.3. Simulation Setup

To compare the $\mathcal{L}_1$ AC and LTI based learning schemes, we will be looking at unknown parameters $\theta(t)$ with $\theta_1(t)$ as the only nonzero element. The reason for this is twofold: First, the Hankel singular values of the states x_1, x_2, x_3, x_4, and x_5 of the balanced realization of $P(s)$ are 910, 454, 172, 170, and 42; respectively. In other words, x_1 has a much higher contribution to the output when compared to other states. Second, by doing

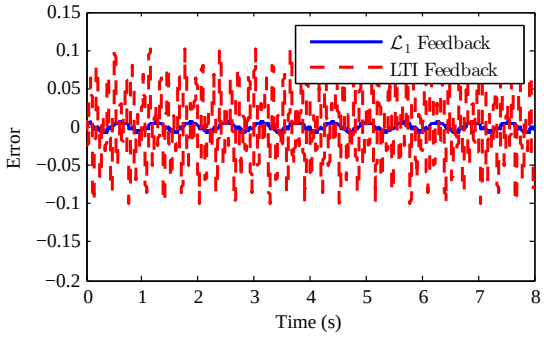

(a) Feedback tracking errors

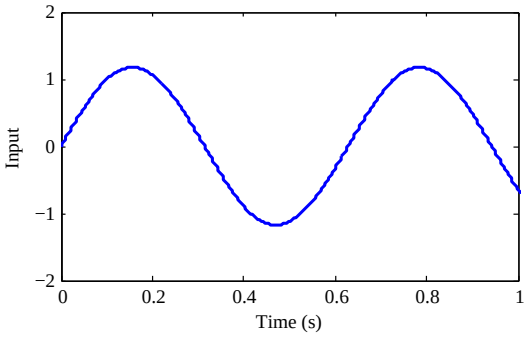

(b) Adaptive control input $u_{ad}(t)$ of the $\mathcal{L}_1$ adaptive controller

Figure 8: Closed loop responses of the $\mathcal{L}_1$ adaptive controller and LTI output controller to $\theta_1(t) = \sin(50t)$ without learning

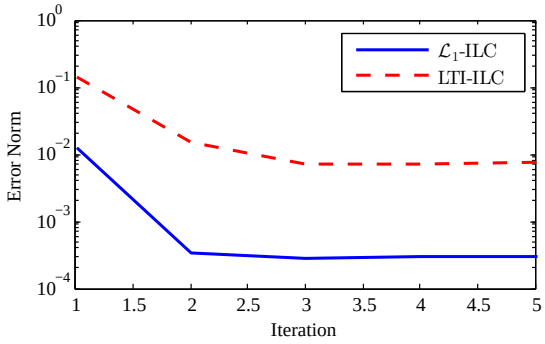

(a) Tracking error reduction through learning

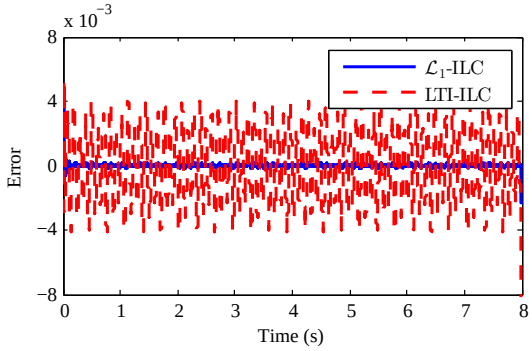

(b) Converged tracking errors

Figure 9: Learning performances of the $\mathcal{L}_1$-ILC and LTI-ILC schemes and for $\theta_1(t) = \sin(50t)$

so we are able to consider large time varying uncertainties without having an excessively conservative robust monotonic convergence condition, stated as

$$\kappa_{tv} \leq \frac{\mu_{tv} - \|Q(-s)Q(s)(1 - L(s)H(s))\|_\infty}{\|Q(-s)Q(s)L(s)H(s)\|_\infty},$$

for $\mu_{tv} \in [0, 1)$, with

$$\kappa_{tv} \triangleq \frac{\theta_{M_\infty}\|1 - C(s)\|_\infty\|H_{x1}(s)\|_\infty}{1 - \theta_{M_\infty}\|G_1(s)\|_\infty},$$

where $H_{x1}(s)$ and $G_1(s)$ are the transfer functions to the first outputs of $H_x(s)$ and $G(s)$, respectively. The readers can verify that the condition guarantees monotonic convergence in the same vein as theorems 4 and 7. More specifically, we have bounds on $H_{x1}(s)$ and $G_1(s)$ since $\theta(t)$ is zero for all elements but $\theta_1(t)$ and $\theta_{M_\infty} < \theta_{M_2}$, $\|H_{x1}(s)\|_\infty \leq \|H_x(s)\|_\infty$ and $\|G_1(s)\|_\infty \leq \|G_x(s)\|_\infty$; and $Q(-s)Q(s)$ due to double filtering, where $Q(-s)$ is the stable *anticausal* counterpart of $Q(s)$. Also note that this further implies $\theta_{M_\infty}\|G_1(s)\|_\infty \leq \theta_{M_2}\|G(s)\|_\infty < 1$.

For the simulation scenarios, we consider the responses of the two schemes to a sinusoidal reference, $r(t) = \sin(10t)$, over periods of 8 seconds, wherein each period defines a trial. At the beginning of each trial, we reset the clock to 0, and reinitiate the process with the updated feedforward signals. To better make our point, we consider *noiseless* measurements for the LTI feedback system.

5.4. Simulation Results

First, we look at the feedback response (without learning) of the two systems to a fast parameter, selected as $\theta_1(t) = \sin(50t)$. We see in figure 8 that $\mathcal{L}_1$ AC clearly outperforms LTI control with an error norm (in the $\mathcal{L}_2$ sense) of 0.0126 against 0.138. We also observe that the $\mathcal{L}_1$ AC input is smooth and devoid of high frequency content from the estimation loop. Then, we study the learning performance of the two schemes and observe in figure 9 that the $\mathcal{L}_1$-ILC scheme performs almost an order of magnitude better than the LTI feedback based system for all iterations. We note that, the converged error of the LTI scheme is much larger than that of the $\mathcal{L}_1$-ILC algorithm with significant effects due to the 50 rad/s feedback uncertainty. We look more closely at the

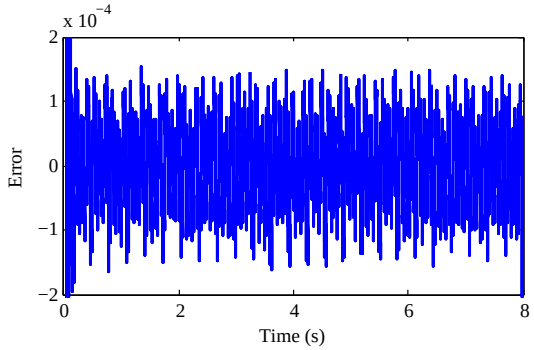

Figure 10: Converged tracking error of the $\mathcal{L}_1$-ILC scheme for $\theta_1(t) = \sin(50t)$

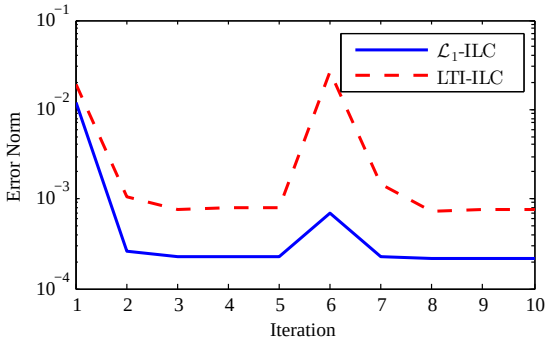

Figure 11: Learning transients of the $\mathcal{L}_1$-ILC and LTI-ILC schemes due to an abrupt change in the sign of $\theta_1(t) = 0.1\sin(50t)$ at the 6$^{\text{th}}$ iteration

converged error of the $\mathcal{L}_1$-ILC architecture in figure 10 and see that the majority of the remaining error comprises of Gaussian noise from the measurements.

Next, we consider two scenarios wherein $\theta_1(t)$ has an abrupt change of sign at the 6$^{\text{th}}$ iteration. In the first scenario, we keep the parameter at the same frequency but decrease the amplitude to 0.1, thus starting the trials with $\theta_1(t) = 0.1\sin(50t)$ and switching to $\theta_1(t) = -0.1\sin(50t)$ at the 6$^{\text{th}}$ iteration. We see in figure 11 that both controllers experience a large transient growth but converge back to equilibrium within a few trials. We also observe that the LTI feedback scheme performs better than before (compare to figure 9) due to decreasing uncertainty, yet the learning performance is still poor when compared to $\mathcal{L}_1$-ILC with larger transients that exceed the original feedback control performance. In the second scenario, we assume a time invariant parameter with a very small amplitude and take $\theta_1(t) = 0.01$, which is changed to $\theta_1(t) = -0.01$ at the 6$^{\text{th}}$ iteration. Figure 12 shows us that the controllers show

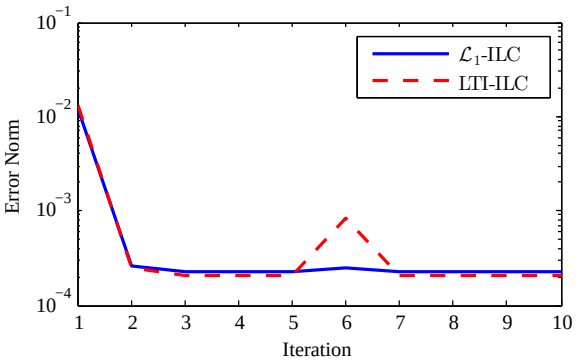

Figure 12: Learning transients of the $\mathcal{L}_1$-ILC and LTI-ILC schemes due to an abrupt change in the sign of $\theta_1(t) = 0.01$ at the 6$^{\text{th}}$ iteration

near identical learning dynamics due to the uncertainty being close to 0. We also see that the converged LTI error is slightly smaller than the $\mathcal{L}_1$ AC error due to the limiting noise factor. However, we observe that the error growth experienced by the LTI feedback based ILC is noticeable, whereas the $\mathcal{L}_1$-ILC system shows negligible change.

Finally, we redirect our attention to figures 9, 11, and 12: We note that the $\mathcal{L}_1$-ILC scheme displays similar performance (in terms of initial and converged errors) regardles of the uncertainty, whereas the LTI feedback based ILC shows approximately an order of magnitude variance in terms of both the initial and converged errors. This clearly indicates the improvement in performance predictability for the $\mathcal{L}_1$-ILC system over the LTI feedback based ILC system.

6. Conclusion

In this paper we presented a combined $\mathcal{L}_1$-ILC scheme for robust precision motion control. $\mathcal{L}_1$ AC was utilized to reduce the effects of parametric variation and increase precision whilst preserving robustness against unmodeled dynamics. This reduction in parametric uncertainty enabled the use of aggressive ILC design to increase system bandwidth and improve tracking performance.

The combined controller is robust against parametric uncertainties *and* unmodeled dynamics, with *high tracking performance over a large bandwidth*. Simulation results on a precision nanopositioner demonstrate that the well posed feedback controller helps us in extracting high performance from ILC and achieve *near perfect tracking* even with information, bandwidth and hardware constraints, which is especially important due

to the complex requirements for high precision tracking even in the presence of parametric uncertainty.

Acknowledgements

This work was supported by startup funds from the University of Michigan.

Appendix A. Intermediate Technical Results

In this section we present some results that are helpful towards evaluating system uncertainties and establishing the relationship of lemma 2. These will be used to show the existence and stability of the feedback operators. In the following discussion, $\mathcal{F}_1 : V_1 \to V_2$ and $\mathcal{F}_2 : V_2 \to V_1$ are operators acting on vector spaces V_1 and V_2.

We first give a generalization of the $\mathcal{L}_1$ norm condition which ensures that the objective of the $\mathcal{L}_1$ AC problem is well defined. While we assume that the inverse exists, the argument is valid regardless of its existence if we think of it as a feedback interconnection. Note that for linear systems, the condition $\|\mathcal{F}_2\mathcal{F}_1\| \leq \phi_2 < 1$ guarantees the existence of a *left inverse* as we show in the proof of theorem 7. This is a special case of the small gain theorem [30, page 218].

Lemma 7. *Assume V_1, V_2 to be endowed with norms such that $\|\mathcal{F}_1\| \leq \phi_1 < \infty$ and $\|\mathcal{F}_2\mathcal{F}_1\| \leq \phi_2 < 1$. Then, $\|\mathcal{F}_1(\mathcal{I} + \mathcal{F}_2\mathcal{F}_1)^{-1}\| \leq \phi_1(1-\phi_2)^{-1}$.*

Proof. Let $\zeta, \xi \in V$ be the input and output vectors of $\mathcal{I} + \mathcal{F}_2\mathcal{F}_1$; respectively. Since $\|\mathcal{F}_2\mathcal{F}_1\| \leq \phi_2 < 1$, we have $\|\xi\| \geq \|\zeta\| - \|\mathcal{F}_2\mathcal{F}_1\|\|\zeta\| \geq (1-\phi_2)\|\zeta\|$ by the reverse triangle inequality. Hence, $\|(\mathcal{I} + \mathcal{F}_2\mathcal{F}_1)^{-1}\| \leq (1-\phi_2)^{-1}$. The result then follows by submultiplicativity.

Let $F_1 \in \mathbb{C}^{m\times n}$, $F_2 \in \mathbb{C}^{n\times m}$. A generalization of the identity $(\mathbb{I} + F_1F_2)^{-1} = \mathbb{I} - F_1(\mathbb{I} + F_2F_1)^{-1}F_2$ to right and left inverses of linear operators is given as follows.

Lemma 8. *Let $\mathcal{F}_1$, $\mathcal{F}_2$ be linear. Then, $(\mathcal{I} + \mathcal{F}_1\mathcal{F}_2)^{-R}$ exists if and only if $(\mathcal{I} + \mathcal{F}_2\mathcal{F}_1)^{-R}$ exists. Moreover, a right inverse of $(\mathcal{I} + \mathcal{F}_1\mathcal{F}_2)$ is $\mathcal{I} - \mathcal{F}_1(\mathcal{I} + \mathcal{F}_2\mathcal{F}_1)^{-R}\mathcal{F}_2$, and a right inverse of $(\mathcal{I} + \mathcal{F}_2\mathcal{F}_1)$ is $\mathcal{I} - \mathcal{F}_2(\mathcal{I} + \mathcal{F}_1\mathcal{F}_2)^{-R}\mathcal{F}_1$. The same relationship holds for left inverses, and consequently inverses.*

Proof. Assume $\mathcal{I} + \mathcal{F}_1\mathcal{F}_2$ is right invertible. Then, $(\mathcal{I} + \mathcal{F}_2\mathcal{F}_1)(\mathcal{I} - \mathcal{F}_2(\mathcal{I} + \mathcal{F}_1\mathcal{F}_2)^{-R}\mathcal{F}_1) = \mathcal{I}$ by direct computation, which shows that $\mathcal{I} - \mathcal{F}_2(\mathcal{I} + \mathcal{F}_1\mathcal{F}_2)^{-1}\mathcal{F}_1$ is a right inverse of $\mathcal{I} + \mathcal{F}_2\mathcal{F}_1$. By interchanging $\mathcal{F}_1$ and $\mathcal{F}_2$, we can show the converse statement. The relationship for left inverses can be shown in the same manner. Since the existence of a right and left inverse is equivalent to the existence of a unique inverse, our proof is complete.

The following shows that the $\mathcal{L}_1$ norm of a system bounds its induced $\mathcal{L}_p$ norm.

Lemma 9. *Let $F(s)$ be a stable causal SISO LTI system. Then for every input $\zeta \in \mathcal{L}_{pe}$, $p \in [1, \infty]$, the output $\xi \in \mathcal{L}_{pe}$ and we have $\|\xi_\tau\|_{\mathcal{L}_p} \leq \|F(s)\|_{\mathcal{L}_1}\|\zeta_\tau\|_{\mathcal{L}_p}$ [30, page 200].*

Appendix B. Proofs of the Main Results

Proof of (Lemma 2). Let $\zeta \in \mathcal{L}^m_{2e}$, $\xi \in \mathcal{L}^n_{2e}$ be the input and output signals; respectively. Then, by lemma 9 $\|(\xi_k)_\tau\|_{\mathcal{L}_2} = \|(\sum_{l=1}^m f_{kl} * \zeta_l)_\tau\|_{\mathcal{L}_2} \leq \sum_{l=1}^m \|f_{kl}\|_{\mathcal{L}_1}\|(\zeta_l)_\tau\|_{\mathcal{L}_2}$, where $*$ denotes convolution. Let

$$\delta_k \triangleq \begin{bmatrix}\|f_{k1}\|_{\mathcal{L}_1} & \|f_{k2}\|_{\mathcal{L}_1} & \dots & \|f_{km}\|_{\mathcal{L}_1}\end{bmatrix}^T,$$
$$\epsilon \triangleq \begin{bmatrix}\|(\zeta_1)_\tau\|_{\mathcal{L}_2} & \|(\zeta_2)_\tau\|_{\mathcal{L}_2} & \dots & \|(\zeta_m)_\tau\|_{\mathcal{L}_2}\end{bmatrix}^T,$$

so $\sum_{l=1}^m \|(f_{kl})_\tau\|_{\mathcal{L}_1}\|(\zeta_l)_\tau\|_{\mathcal{L}_2} = \delta_k^T\epsilon$. Now the Cauchy-Schwarz inequality implies $\delta_k^T\epsilon \leq \|\delta_k\|_2\|\epsilon\|_2$, hence we get $\sum_{l=1}^m \|(f_{kl})_\tau\|_{\mathcal{L}_1}\|(\zeta_l)_\tau\|_{\mathcal{L}_2} \leq \|\delta_k\|_2\|\epsilon\|_2 \leq \|\delta_k\|_1\|\epsilon\|_2$. Moreover, $\|\delta_k\|_1 \leq \|F(s)\|_{\mathcal{L}_1}$ and $\|\epsilon\|_2 = \|\zeta_\tau\|_{\mathcal{L}_2}$ by definition, which imply $\|(\xi_k)_\tau\|_{\mathcal{L}_2} \leq \|F(s)\|_{\mathcal{L}_1}\|\zeta_\tau\|_{\mathcal{L}_2}$. Thus, $\|\xi_\tau\|_{\mathcal{L}_2} \leq \sqrt{n}\|F(s)\|_{\mathcal{L}_1}\|\zeta_\tau\|_{\mathcal{L}_2}$. By theorem 1, it follows that $\|F(s)\|_\infty \leq \sqrt{n}\|F(s)\|_{\mathcal{L}_1}$.

Proof of (Theorem 4). By the Cauchy-Schwarz inequality, $|\theta^T G(j\omega)| \leq \|\theta\|_2\|G(j\omega)\|_2 \leq \theta_{M_2}\|G(s)\|_\infty$, $\forall\omega \in \mathbb{R}$. Note that $\theta_{M_2} = \sqrt{n}\theta_M$, so by lemma 2, we have $\|\theta^T G(s)\|_\infty \leq \theta_{M_2}\|G(s)\|_\infty \leq \theta_{M_1}\|G(s)\|_{\mathcal{L}_1} < 1$. Let $G_\theta(s) \triangleq (\theta^T G(s))/(1 - \theta^T G(s))$, which implies $\bar{H}(s) = H(s)(1 + G_\theta(s))$. By lemma 7,

$$|G_\theta(j\omega)| \leq \|G_\theta(s)\|_\infty \leq \frac{\theta_{M_2}\|G(s)\|_\infty}{1 - \theta_{M_2}\|G(s)\|_\infty} = \kappa,$$

$\forall\omega \in \mathbb{R}$. Assume there exists $\mu \in [0, 1)$ such that

$$|Q(j\omega)(1 - L(j\omega)\bar{H}(j\omega))| \leq$$
$$|Q(j\omega)\|(1-L(j\omega)H(j\omega))|+\kappa|Q(j\omega)\|(L(j\omega)\|H(j\omega)| \leq \mu,$$

$\forall\omega \in \mathbb{R}$. But then, this is equivalent to (9).

Proof of (Lemma 4). We extend $\mathcal{L}_1$ to include complex transfer functions and note that the inverse Laplace transform of $1/(s + p)$ is $e^{-pt}1(t)$, which implies

$\|(s+p)^{-1}\|_{\mathcal{L}_1} = 1/\operatorname{Re}(p)$, $\forall p : \operatorname{Re}(p) > 0$. Without loss of generality, assume $m = n-1$. Then we have,

$$\begin{aligned}\|F(s)\|_{\mathcal{L}_1} &\leq \|\frac{1}{s+p_n}\|_{\mathcal{L}_1} \prod_{k=1}^{n-1} \|\frac{s+z_k}{s+p_k}\|_{\mathcal{L}_1} \\ &\leq \frac{1}{\operatorname{Re}(p_n)} \prod_{k=1}^{n-1} 1 + \frac{|z_k|}{\operatorname{Re}(p_k)} + \frac{|p_k|}{\operatorname{Re}(p_k)}.\end{aligned}$$

Now the assumption $\arg(p_k) \in [\psi, 2\pi - \psi]$ implies $1/\operatorname{Re}(p_k) \to 0$ as $|p_k| \to \infty$ and $|p_k|/\operatorname{Re}(p_k)$ is bounded for $p_k \neq 0$. It follows that $1 + |z_k|/\operatorname{Re}(p_k) + |p_k|/\operatorname{Re}(p_k)$ is $O(1)$ for $k = 1, 2, \ldots, n-1$. Since $1/\operatorname{Re}(p_n) \to 0$, the result follows.

Proof of (Theorem 7). The proof follows the same ideas of theorem 4. We first show that the $\mathcal{L}_2$ gain of $\mathcal{W}\mathcal{G}_m$ is less than 1 due to the $\mathcal{L}_1$ norm condition. Note that $\mathcal{W}$ is made up of 3 cascaded systems (14) with the first one being LTI. The readers can therefore easily verify $\Psi \triangleq M_2\|T(s)A_T G_m(s)\|_\infty$ to be an upper bound on the induced $\mathcal{L}_2$ norm of $\mathcal{W}\mathcal{G}_m$. From lemma 2 and the equality $\theta_{M_1} = \sqrt{n}\theta_{M_2}$ it follows that $\Psi \leq M\|G_m(s)\|_{\mathcal{L}_1} < 1$.

Since the $\mathcal{L}_2$ gain of $\mathcal{W}\mathcal{G}_m$ is less than 1, it follows that $\mathcal{I} - \mathcal{W}\mathcal{G}_m$ is nonsingular, which implies it is one-to-one. Hence $\mathcal{I} - \mathcal{W}\mathcal{G}_m$ has a left inverse, with $\mathcal{L}_2$ gain less than $1 - \Psi$ by lemma 7.

Let $\mathcal{G}_{m\theta} \triangleq (\mathcal{I} - \mathcal{C})(\mathcal{I} - \mathcal{W}\mathcal{G}_m)^{-L}\mathcal{W}\mathcal{H}_{xm}$, where $\mathcal{H}_{xm}$ is $H_{xm}(s)$ in operator notation. It follows that an upper bound on the $\mathcal{L}_2$ gain of $\mathcal{G}_{m\theta}$ is

$$\frac{M_2\|T(s)A_T H_{xm}(s)\|_\infty \|1 - C(s)\|_\infty}{1 - M_2\|T(s)A_T G_m(s)\|_\infty},$$

which is equal to $\kappa_{m_{tv}}$ by definition. Moreover, by lemma 8, the mapping $\bar{\mathcal{H}}_m$ from v_i to y_i is given by $\bar{\mathcal{H}}_m = \mathcal{H}_m(\mathcal{I} + \mathcal{G}_{m\theta})$. Now let $\mathcal{Q}$, $\mathcal{L}$ be $Q(s)$ and $L(s)$ in operator notation; respectively. Assume there exists $\mu_{m_{tv}} \in [0, 1)$ such that,

$$\begin{aligned}\|\mathcal{Q}(\mathcal{I} - \mathcal{L}\bar{\mathcal{H}}_m)\|_{\mathcal{L}_2} &\leq \|\mathcal{Q}(\mathcal{I} - \mathcal{L}\mathcal{H}_m)\|_{\mathcal{L}_2} + \kappa_{m_{tv}}\|\mathcal{Q}\mathcal{L}\mathcal{H}_m\|_{\mathcal{L}_2} \\ &\leq \mu_{m_{tv}}.\end{aligned}$$

But then, this is equivalent to (25) by theorem 1.

Remark 7. The existence of $(\mathcal{I} - \mathcal{W}\mathcal{G}_m)^{-L}$ can also be proven by $M\|G_m(s)\|_{\mathcal{L}_1} < 1$ or any norm that satisfies the small gain condition since this implies that $\mathcal{I} - \mathcal{W}\mathcal{G}_m$ is nonsingular. This property would be useful if it cannot be shown that the $\mathcal{L}_2$ gain is less than the $\mathcal{L}_1$ norm. For instance, if $\|F(s)\|_{\mathcal{L}_1} < 1$, but $\|F(s)\|_\infty < 1$ is not necessarily true, $\|(\mathbb{I} - F(s))^{-1}\|_\infty \leq \sqrt{n}/(1 - \|F(s)\|_{\mathcal{L}_1})$ by lemmas 2 and 7. Obviously, this would lead to a more restrictive robust convergence condition.

Appendix C. $\mathcal{L}_1$ Adaptive Output Feedback Controller Definitions

We list the variables that are used in section 4 below. The readers can refer to [29] for the original definitions, we provide several modifications to account for the addition of $v_i(t)$ in the adaptive controller.

$$\begin{aligned}\rho_1 \triangleq (&|k_g|\|H_{xm}(s)C(s)\|_{\mathcal{L}_1}\|r\|_{\mathcal{L}_\infty} + \|H_{xm}(s)\|_{\mathcal{L}_1}\|v_i\|_{\mathcal{L}_\infty} \\ &+ \|G_m(s)\|_{\mathcal{L}_1}(\|\sigma_m\|_{\mathcal{L}_\infty} + M\rho_2))/(1 - \|G_m(s)\|_{\mathcal{L}_1}M),\end{aligned}$$

where $\rho_2 \triangleq \|x_{ref_2}\|_{\mathcal{L}_\infty}$; and $x_{ref_2}(t)$ is defined according to $\dot{x}_{ref_2}(t) = A_m x_{ref_2}(t)$, $x_{ref_2}(0) = \hat{x}_{in}$. Let $\rho \triangleq \rho_1 + \rho_2$ and $\bar{\Delta} \triangleq \Delta_m + M(\rho + \bar{\gamma}\|C(s)\|_{\mathcal{L}_1}/(1 - \|G_m(s)\|_{\mathcal{L}_1}M))$, where $\bar{\gamma} > 0$ is arbitrary. Define

$$\beta_1 \triangleq \beta_{01}\frac{\|C(s)\|_{\mathcal{L}_1}}{1 - \|G_m(s)\|_{\mathcal{L}_1}M}, \quad \beta_2 \triangleq \beta_{02} + \beta_{01}\rho,$$

$$\beta_{01} \triangleq 4\bar{\Delta}M\left(d_\theta/\theta_{M_1} + \|A_m\|_{\mathcal{L}_1} + \|b_m\|_{\mathcal{L}_1}M\right),$$

$$\begin{aligned}\beta_{02} \triangleq 4\bar{\Delta}(&d_{\sigma_m} + M\|b_m\|_{\mathcal{L}_1}(\|C(s)\|_{\mathcal{L}_1}(|k_g|\|r\|_{\mathcal{L}_\infty} + \bar{\Delta}) + \\ &\|v_i\|_{\mathcal{L}_\infty} + \Delta_m)),\end{aligned}$$

$$\beta_3 \triangleq \frac{\lambda_{max}(P_m)}{\lambda_{min}(Z_m)}\beta_1, \quad \beta_4 \triangleq 4\bar{\Delta}^2 + \frac{\lambda_{max}(P_m)}{\lambda_{min}(Z_m)}\beta_2.$$

The transient bounds of the controller are given by

$$\gamma_0 \triangleq \sqrt{\alpha\beta_4/(\Gamma_c\lambda_{min}(P_m))}$$

$$\gamma_1 \triangleq \gamma_0\|C(s)\|_{\mathcal{L}_1}/(1 - \|G_m(s)\|_{\mathcal{L}_1}M),$$

$$\gamma_2 \triangleq M\|C(s)\|_{\mathcal{L}_1}\gamma_1 + \|(C(s)/(c_o^T H_{xm}(s)))c_o^T\|_{\mathcal{L}_1}\gamma_0,$$

where $c_o \in \mathbb{R}^n$ is arbitrary such that $c_o^T H_{xm}(s)$ is minimum phase and has relative degree 1.

References

[1] Bristow D., Tharayil M., Alleyne A. A survey of iterative learning control. Control Systems, IEEE2006;26(3):96–114. doi:10.1109/MCS.2006.1636313.

[2] Moore K.L. Iterative Learning Control for Deterministic Systems. London: Springer-Verlag; 1993.

[3] Ahn H.S., Chen Y.Q., Moore K. Iterative learning control: Brief survey and categorization. Systems, Man, and Cybernetics, Part C: Applications and Reviews, IEEE Transactions on2007;37(6):1099–121. doi:10.1109/TSMCC.2007.905759.

[4] De Roover D., Bosgra O.H. Synthesis of robust multivariable iterative learning controllers with application to a wafer stage motion system. International Journal of Control2000;73(10):968–79. doi:10.1080/002071700405923.

[5] Moon J.H., Doh T.Y., Chung M.J. A robust approach to iterative learning control design for uncertain systems. Automatica1998;34(8):1001 –4. doi:http://dx.doi.org/10.1016/S0005-1098(98)00028-4.

[6] van de Wijdeven J., Donkers T., Bosgra O. Iterative learning control for uncertain systems: Robust monotonic convergence analysis. Automatica2009;45(10):2383 –91. doi:http://dx.doi.org/10.1016/j.automatica.2009.06.033.

[7] Helfrich B., Lee C., Bristow D., Xiao X., Dong J., Alleyne A., et al. Combined $\mathcal{H}_\infty$-feedback control and iterative learning control design with application to nanopositioning systems. Control Systems Technology, IEEE Transactions on2010;18(2):336–51. doi:10.1109/TCST.2009.2018835.

[8] Ahn H.S., Moore K.L., Chen Y. Stability analysis of discrete-time iterative learning control systems with interval uncertainty. Automatica2007;43(5):892 – 902. doi:http://dx.doi.org/10.1016/j.automatica.2006.11.020.

[9] Tayebi A. Adaptive iterative learning control for robot manipulators. Automatica2004;40(7):1195 –203. doi:http://dx.doi.org/10.1016/j.automatica.2004.01.026.

[10] Sun D., Mills J. High-accuracy trajectory tracking of industrial robot manipulator using adaptive-learning scheme. In: American Control Conference, 1999. Proceedings of the 1999; vol. 3. 1999, p. 1935–1939 vol.3. doi:10.1109/ACC.1999.786195.

[11] Tayebi A. Model reference adaptive iterative learning control for linear systems. International Journal of Adaptive Control and Signal Processing2006;20(9):475–89. doi:10.1002/acs.913.

[12] Chien C.J., Yao C.Y. Iterative learning of model reference adaptive controller for uncertain nonlinear systems with only output measurement. Automatica2004;40(5):855 –64. doi:http://dx.doi.org/10.1016/j.automatica.2003.12.009.

[13] Choi J., Lee J. Adaptive iterative learning control of uncertain robotic systems. IEE Proceedings - Control Theory and Applications2000;147:217–223(6).

[14] French M., Rogers E. Non-linear iterative learning by an adaptive lyapunov technique. International Journal of Control2000;73(10):840–50. doi:10.1080/002071700405824.

[15] Owens D.H., Munde G. Error convergence in an adaptive iterative learning controller. International Journal of Control2000;73(10):851–7. doi:10.1080/002071700405833.

[16] Rohrs C., Valavani L., Athans M., Stein G. Robustness of continuous-time adaptive control algorithms in the presence of unmodeled dynamics. Automatic Control, IEEE Transactions on1985;30(9):881–9. doi:10.1109/TAC.1985.1104070.

[17] Cao C., Hovakimyan N. $\mathcal{L}_1$ Adaptive Control Theory: Guaranteed Robustness with Fast Adaptation. Philadelphia, PA: Society for Industrial and Applied Mathematics; 2010.

[18] Devasia S., Eleftheriou E., Moheimani S.O.R. A survey of control issues in nanopositioning. Control Systems Technology, IEEE Transactions on2007;15(5):802–23. doi:10.1109/TCST.2007.903345.

[19] Freudenberg J.S., Looze D.P. Frequency Domain Properties of Scalar and Multivariable Feedback Systems. Berlin: Springer-Verlag; 1988.

[20] Stein G. Respect the unstable. Control Systems, IEEE2003;23(4):12–25. doi:10.1109/MCS.2003.1213600.

[21] Barton K., Mishra S., Xargay E. Robust iterative learning control: $\mathcal{L}_1$ adaptive feedback control in an ILC framework. In: American Control Conference (ACC), 2011. 2011, p. 3663–8.

[22] Altin B., Barton K. $\mathcal{L}_1$ adaptive control in an iterative learning control framework: Stability, robustness and design trade-offs. In: American Control Conference (ACC), 2013. 2013, p. 6697–702.

[23] Altın B., Barton K. $\mathcal{L}_1$ adaptive control in an iterative learning control framework for precision nanopositioning. In: Proc. of the ASPE Spring Top. Meet.; vol. 55. 2013, p. 88–93.

[24] Zhou K., Doyle J.C., Glover K. Robust and Optimal Control. Eaglewood Cliffs, NJ: Prentice-Hall; 1996.

[25] Cao C., Hovakimyan N. Stability margins of $\mathcal{L}_1$ adaptive control architecture. Automatic Control, IEEE Transactions on2010;55(2):480–7. doi:10.1109/TAC.2009.2037384.

[26] Cao C., Hovakimyan N. Design and analysis of a novel $\mathcal{L}_1$ adaptive controller, part i: Control signal and asymptotic stability. In: American Control Conference, 2006. 2006, p. 3397–402. doi:10.1109/ACC.2006.1657243.

[27] Pomet J.B., Praly L. Adaptive nonlinear regulation: estimation from the Lyapunov equation. Automatic Control, IEEE Transactions on1992;37(6):729–40. doi:10.1109/9.256328.

[28] Verwoerd M., Meinsma G., De Vries T.J.A. On the use of noncausal LTI operators in iterative learning control. In: Decision and Control, 2002, Proceedings of the 41st IEEE Conference on; vol. 3. 2002, p. 3362–3366 vol.3. doi:10.1109/CDC.2002.1184394.

[29] Cao C., Hovakimyan N. $\mathcal{L}_1$ adaptive output feedback controller for systems with time-varying unknown parameters and bounded disturbances. In: American Control Conference, 2007. ACC '07. 2007, p. 486–91. doi:10.1109/ACC.2007.4282994.

[30] Khalil H.K. Nonlinear Systems. Eaglewood Cliffs, NJ: Prentice-Hall; 2002.

[31] Parmar G., Barton K., Awtar S. Large dynamic range nanopositioning using iterative learning control. Precision Engineering2013;doi:http://dx.doi.org/10.1016/j.precisioneng.2013.07.003.